International Journal of Non-Linear Mechanics xxx (xxxx) xxx–xxx

Contents lists available at ScienceDirect

International Journal of Non-Linear Mechanics

journal homepage: www.elsevier.com/locate/nlm

Energy harvesting from pendulum oscillations

Michał Marszal[a], Błażej Witkowski[b,c], Krzysztof Jankowski[a], Przemysław Perlikowski[a,*], Tomasz Kapitaniak[a]

[a] Division of Dynamics, Lodz University of Technology, ul. Stefanowskiego 1/15, 90-924 Lodz, Poland
[b] Department of Mechanics and Mechatronics, Gdansk University of Technology, ul. Narutowicza 11/12, 80-233 Gdansk, Poland
[c] Institute of Machine Tools and Production Engineering, Lodz University of Technology, ul. Stefanowskiego 15, 90-924 Lodz, Poland

ARTICLE INFO

Keywords:
Energy harvesting
Pendulum

ABSTRACT

In this work we analyse the possibility of energy harvesting from the vibration of the environment. The investigations are performed using experimental rig, which consists of a parametrically forced pendulum and an energy harvester, and the mathematical model developed based on the experimental rig. Numerical studies focus on the oscillating motion of pendulum in 2:1 resonance and show good agreement with experimental results. We present that the energy harvesting is possible and is more efficient for shorter reduced length of the pendulum, as proved numerically and experimentally.

1. Introduction

Pendulum is the most fundamental example of mechanical oscillator. It has drawn attention of scientists since ages, just to mention Galileo [1] or Huygens [2]. The basic application of pendulum is to measure the time, as for small swing amplitude φ_0 the period T depends only on the length of the pendulum l, which can be formulated as follows:

$$T = 2\pi\sqrt{\frac{l}{g}} \quad \varphi_0 \ll 1. \tag{1}$$

The pendulum has a simple design principle, yet can exhibit very complex dynamics [3] and has been widely used as a building block in complex nonlinear systems [4–13]. When the pendulum is subjected to excitation with angular frequency ω two times larger than the natural frequency Ω, a 2:1 parametric resonance occurs. Such a property of the pendulum has convinced scientists to investigate possible application of pendulum in energy harvesting. Most of the ideas involve using sea waves as source of excitation. The pendulum system, placed on floating structure, oscillates or rotates transforming mechanical energy into electrical energy [14,15]. The topic of rotating solutions of parametrically excited pendulum is addressed in [16], while the optimization of energy extraction from such a system is presented in [17]. Energy extraction from rotary motion of pendulum subjected to stochastic wave excitation is described in [18]. Laboratory experiments in wave flume are performed in [19], as well as in [20] where authors test 1:45 scaled model of energy harvesting device, prepare simple analytical model and make usability study based on the oceanographic data for Italian coastline. However, when using sea waves as an excitation source for the pendulum system, one should construct long pendulum in order to obtain 2:1 resonance. For example a period of sea waves $T_w = 3$ [s] corresponds to almost nine meters long pendulum (according to [21] ordinary gravity waves periods span from 1 [s] to 30 [s]). The problem of obtaining low natural frequency of pendulum is addressed in [22], where authors propose a system of n equally spaced pendula forming a ring with a common pivot point, which eliminates the direct dependence of pendulum length on its natural period. The concept has been further developed in [23–25]. The other approach presented in many works is vertical axis pendulum, where central pivoted pendulum on floating structure rotates around vertical axis. The first patent for device using this principle was issued back in 1966 [26]. Nowadays patents for modern designs are owned by Neptune Wave Power LLC [27,28] and Wello Oy [29]. Papers [30,31] discuss modelling and optimization of vertical axis pendulum wave energy generator. Energy harvesting from the point of view of vibration absorption is shown in [32].

We propose a simple device to harvest the energy from oscillating environments based on pendulum oscillations in 2:1 parametric resonance. The mechanical energy of pendulum is transformed by power generator into electrical energy. This paper is organized as follows: In Section 2 mathematical model and working principles of the investigated system are presented, which includes the pendulum, transmission system, as well as DC power generator. In Section 3 the results of the experimental and numerical study are presented, while the last Section 4 summarizes the obtained results.

* Corresponding author.
E-mail address: przemyslaw.perlikowski@p.lodz.pl (P. Perlikowski).

http://dx.doi.org/10.1016/j.ijnonlinmec.2017.03.022
Received 11 May 2016; Received in revised form 2 March 2017; Accepted 15 March 2017

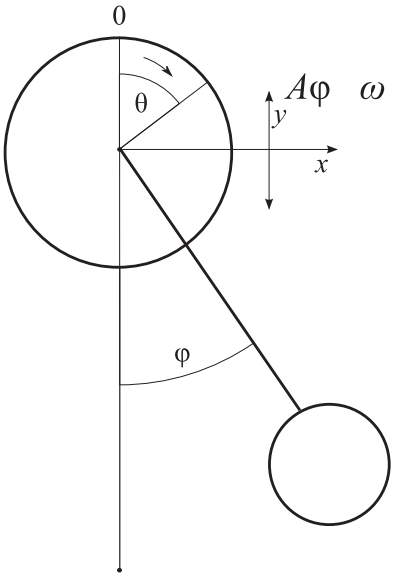

Fig. 1. Schematics of the mathematical model of the system (φ - angular position of pendulum, θ - angular position of flywheel, $A\cos\omega t$ kinematic vertical excitation.

2. Investigated system and working principles

A system of physical pendulum excited vertically is investigated, as the proof of possible energy harvesting from the pendulum oscillations. The oscillations of the pendulum power a electric generator. The torque of pendulum is transferred by the system of gears, a freewheel and a small precision coupling attached to the electric generator shaft.

The mathematical model is developed for already existing construction. The pendulum structure consists of a rod, weight discs, flywheel with gear systems, a hub with freewheel mechanism, a precision coupling and a small electric generator. The flywheel with gear system is connected to pendulum shaft using freewheel mechanism. Freewheel transfers motion of the pendulum to the gear system, which eventually is transferred to the electric generator, wherein mechanical energy is transformed into electric current. The schematics of analytical model, along with principles explaining how the phase variables are chosen, is presented in Fig. 1, while the device is illustrated in Fig. 2(a). The experimental set-up is photographed in Fig. 3.

The system can be represented mathematically by the following set of equations:

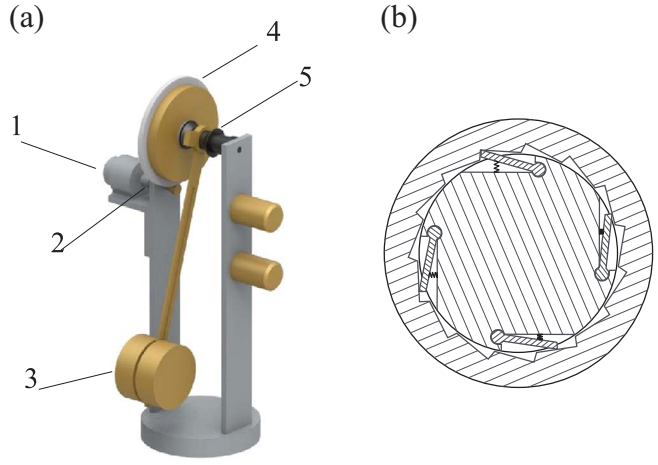

Fig. 2. (a) Model of the investigated pendulum: (1) electric generator, (2) precision coupling, (3) pendulum, (4) flywheel with gear system, (5) hub with ratcheting freewheel mechanism. (b) Cross section of a freewheel mechanism.

$$\begin{cases} I_1\ddot{\varphi} + c_1\dot{\varphi} + m\omega^2 Al\cos(\omega t)\sin\varphi + mgl\sin\varphi = 0 \\ I_2\ddot{\theta} + c_2\dot{\theta} + sgn(\dot{\theta})M_f = 0 \end{cases} \tag{2}$$

where: φ - angular position of pendulum, θ - angular position of flywheel, I_1, I_2 - moment of inertia of pendulum and reduced moment of inertia of freewheel, gear box, shaft and electric generator; m - mass of pendulum, l - distance from centre of gravity to pivot axis; c_1, c_2 - viscous angular damping coefficients, M_f - friction torque; A - amplitude of vertical excitation, ω - frequency of excitation; t - time, g - gravity acceleration. Overdots stand for derivatives with respect to time t. The electrical part of the model is described in further part of this paper.

The freewheel provides simple directional coupling and enables mechanical separation of driveshaft from the driven shaft in certain circumstances, i.e., it disengages when driveshaft (input) rotates slower than the driven shaft (output). Freewheel is a common mechanism encountered in vehicles, as it prevents reversing the energy flow in the system (e.g. vehicle wheels going downhill do not power the motor, which is definitely not desirable). While disengaged, output shaft can rotate freely (*freewheeling*) using energy from its momentum to keep angular motion. Freewheel mechanism is depicted in the Fig. 2(a). It consists of two gears placed one inside the other. The inside gear is equipped with teeth and spring-loaded pawls mechanism, working based on ratchet principle. The outside gear has cut indentions to match the teeth. Should the inside gear rotate faster then outside gear the engagement occurs. In freewheel devices usually two or more pawls are applied to obtain better reliability and decrease the wear. However, it is rare that more than two pawls can engage simultaneously. In the investigated system the freewheel model is simplified by assuming only single pawl and $n_f = 16$ teeth in mechanism. As the teeth are equally spaced on disk perimeter, the engagement can occur if the amplitude of pendulum (driving shaft) is greater than critical value $\varphi_{critical}$, which can be calculated from the number of teeth n_f in mechanism.

$$\varphi_{critical} = \frac{2\pi}{n_f} \tag{3}$$

Engagement takes place only if the following conditions are fulfilled:

$$\dot{\varphi} > \dot{\theta} \quad \wedge \quad \exists_{k\in\{1,..,16\}} \; \varphi = k\varphi_{critical} \tag{4}$$

At the engagement instance the velocities of both shafts are calculated using Newtonian impact theory with coefficient of restitution C_R. The system can be then considered as a body with one degree of freedom, as shown in Eq. (5). The moment of inertia (and viscous damping coefficient) is equal to the moment of inertia of the pendulum and the rest of the system reduced to the axis of the pendulum.

$$(I_1 + I_2)\,\ddot{\varphi} + (c_1 + c_2)\,\dot{\varphi} + m\omega^2 A\, l\cos(\omega t)\sin\varphi + mgl\sin\varphi + M_f = 0 \tag{5}$$

The electromotive force ε generated by the DC generator is proportional to the input speed on the generator shaft, thus:

$$\varepsilon = K_e z\dot{\theta} \tag{6}$$

where K_e - generator constant, z - gear ratio. DC generator is model by three elements connected in series (i.e., generator, resistor - representing armature resistance R_{int}, coil - representing armature inductance L). R_L is a electrical load connected to the power source. It is possible to choose between two values of resistance R_L applied in the system, as seen in the Fig. 4. Applying Kirchhoff voltage law for the circuit one obtains:

$$K_e z\dot{\theta} - i(R_{int} + R_L) - L\frac{\mathrm{d}i}{\mathrm{d}t} = 0, \tag{7}$$

where i is the current flowing through the circuit. Although the DC generator is applied the input speed on generator shaft is not constant, thus the need of including the armature inductance term in Eq. (7) The instantaneous power P generated on resistor R_L is then equal to:

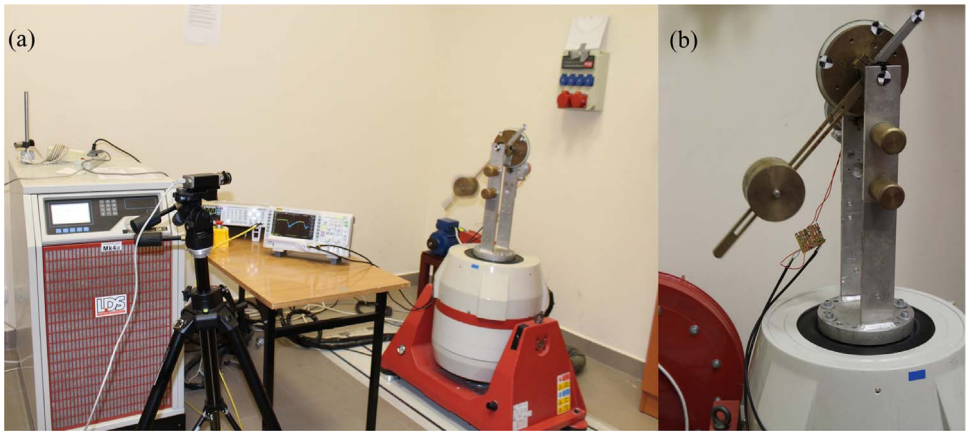

Fig. 3. Experimental set-up (a) and zoom in on the pendulum (b).

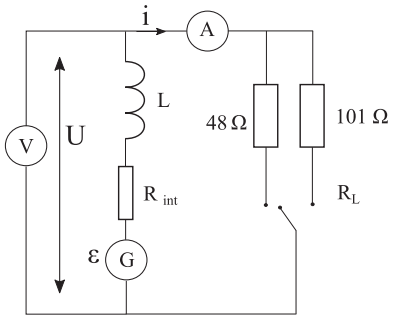

Fig. 4. Scheme of electrical circuit.

$$P = i^2 R_L. \tag{8}$$

Effective power P_e over time interval $\Delta t = t_2 - t_1$ is given by following formula:

$$P_e = \frac{\int_{t_1}^{t_2} P(t)dt}{\Delta t}. \tag{9}$$

Eq. (7) combined with Eq. (2) form the system of ODE - Eq. (10), which describes mechanical and electrical properties of the system.

$$I_1\ddot{\varphi} + c_1\dot{\varphi} + m\omega^2 A\, l \cos(\omega t)\sin\varphi + mgl\sin\varphi = 0 \tag{10a}$$

$$I_2\ddot{\theta} + c_2\dot{\theta} + sgn(\dot{\theta})M_f = 0 \tag{10b}$$

$$K_e z\dot{\theta} - i(R_{int} + R_L) - L\frac{\mathrm{d}i}{\mathrm{d}t} = 0 \tag{10c}$$

The pendulum oscillations can be observed in the region of 2:1 parametric resonance when the excitation frequency doubles the natural frequency of the pendulum. In the considered system, a physical pendulum is used, which can be treated as a mathematical pendulum with mass point at a distance $l_r = I_1/ml$ (reduced length) from the pivot axis. Due to the sine term in equation of motion of simple mathematical pendulum, it is possible to apply small-angle approximation, which yields to straightforward relation between natural frequency ω_0, natural period T_0 and the reduced length of the pendulum l_r, namely, $\omega_0 = \sqrt{g/l_r}$, $T_0 = 2\pi/\omega_0$. On the other hand these relations are not valid for larger amplitudes, where one needs to take into account additional dependence on amplitude of oscillations. To address this issue, a power series approximation of elliptical integral can be applied. Another factor influencing the frequency of oscillations is damping. For damped systems, the frequency of oscillations ω_d slightly changes:

$$\omega_d = \sqrt{\omega_0^2 - \left(\frac{c}{2m}\right)^2} \tag{11}$$

Summarizing the above mentioned dependencies one can conclude that natural period of pendulum depends on its reduced length, amplitude of oscillation and also damping. The parametric resonance in that particular range of amplitude of excitation A, occurs only at small parameter space (see Fig. 5). The system is very sensitive to changes in the excitation period and it is very easy to jump out of the resonance state. In order to set the pendulum oscillating in amplitude ranges about 0.87 [rad], the system is started in parametric resonance for small amplitudes. As the amplitude grows, the period of excitation is slowly increased, so that it matches the new natural period of oscillation. In experiment this was done manually without any control system. It is possible to obtain amplitudes around $\pi/2$ [rad], but due to equipment limitations (i.e., high dynamic torque on the pendulum mounting) we decided to set level of target amplitude at 0.87 [rad].

The electromotive force generated, depends on the input angular velocity on the generator shaft (Eq. (6)), which reaches the largest values for pendula with high natural frequency. On the other hand, the longer the pendulum is, the larger driving torque is produced to overcome damping and friction. For that reason, the influence of the l_r on the effective generated power is investigated in Section 3.3.

In experiment two different values of loading resistors R_L are applied. Different electrical resistance in the circuit influences the mechanical properties of the model. The smaller the resistance the greater the generated current, which yields to greater Lorentz force inside the generator, which opposes the movement of generator shaft.

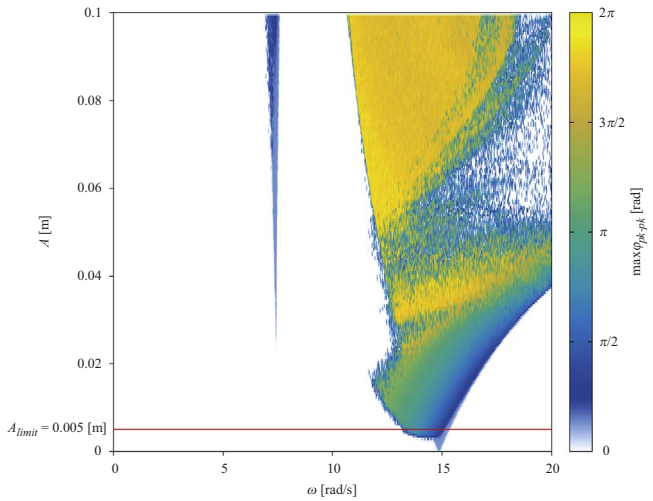

Fig. 5. Maximum peak-to-peak amplitude $\max\varphi_{pk-pk}$ (colour) in (ω, A) parameter space. Red line represents laboratory limit A_{limit}. $l_{red} = 0.178$ [m], $R_L = 101$ [Ω]. Initial conditions for each point on (ω, A) plane: $\varphi = -\pi/3$, $\dot{\varphi} = 0$, $\theta = 0$, $\dot{\theta} = 0$, $i = 0$. (For interpretation of the references to color in this figure legend, the reader is referred to the web version of this article).

Table 1
Values of parameters applied in the mathematical model based on experimental measurements.

I_1	I_2	m	C_R
$6.46 \cdot 10^{-1}$ [kgm^2]	$7.96 \cdot 10^{-3}$ [kgm^2]	5.07 [kg]	0.3
M_f	A	z	
$4.29 \cdot 10^{-2}$ [Nm]	5 [mm]	10	
L	K_e	R_{int}	
13.5 [mH]	$1.41 \cdot 10^{-1}$ [Vs/rad]	15.4 [Ω]	
c_1	c_2 for $R_L = 48$ [Ω]	c_2 for $R_L = 101$ [Ω]	
$9.49 \cdot 10^{-3}$ [kgm^2/s]	$2.81 \cdot 10^{-2}$ [kgm^2/s]	$1.97 \cdot 10^{-2}$ [kgm^2/s]	

This property of the generator is implemented by applying different values of damping coefficient c_2 for each electrical resistance (see Table 1). We determine values of c_2 based on dissipation of the energy during free rotation of system moment of inertia I_2 (at the time of measurements of the damping coefficient the pendulum is decoupled). All values of parameters in Table 1 are determined based upon the measurements performed with the experimental system.

3. Results and discussion

In this section, the results of numerical computation, as well as experimental measurements of the investigated system are presented. Our main goals are to achieve comparable qualitative behaviour of the mathematical model with a real laboratory rig and to perform parameters studies on the influence of reduced length of pendulum on the obtained effective power. Mathematical model is developed from already existing prototype, so it is crucial to identify the parameters and phenomena governing the system.

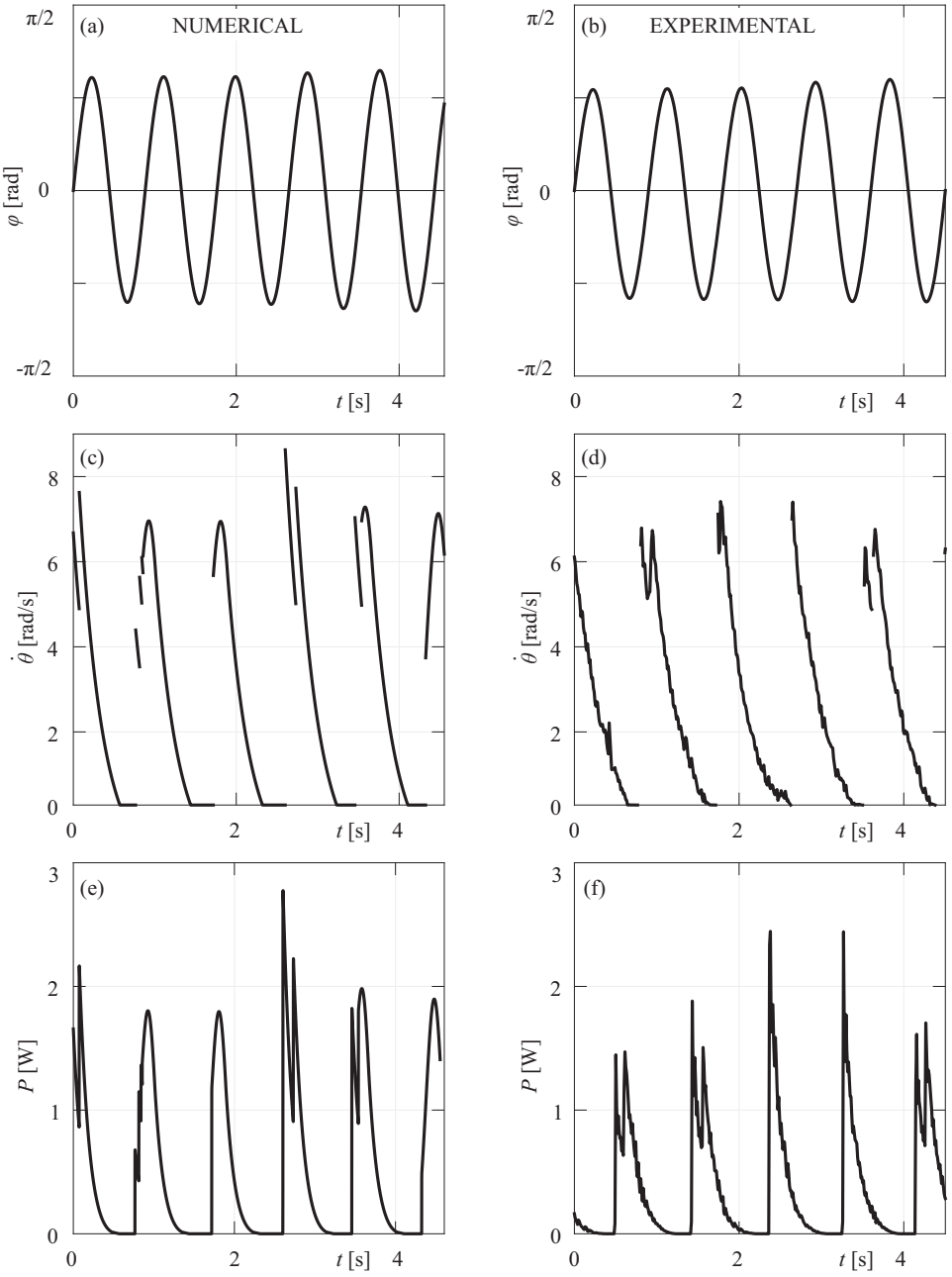

Fig. 6. Time diagrams for numerical and experimental model: angular position of pendulum φ (a) numerical (b) experimental, angular velocity of flywheel $\dot{\theta}$ (c) numerical (d) experimental, instantaneous power P_i (e) numerical (f) experimental. System parameters values: $l = 0.157$ [m], $l_r = 0.177$ [m], $\omega = 14.16$ [rad/s], $R_L = 48$ [Ω].

3.1. Numerical results

The integration of set of ODE (Eq. (10)) is performed using Runge-Kutta-Fehlberg 45 method, wherein values of system parameters and geometry are kept constant throughout the whole experiment. The values of viscous damping coefficients are measured in the experimental system and used in the mathematical model. The coefficient of restitution $C_R = 0.3$ is calculated, based upon velocities and moments of inertia of the pendulum and the flywheel before and after impact. Freewheel mechanism consists of $n_f = 16$ teeth, resulting in the critical angle $\varphi_{critical} = 0.392$ [rad] (see Eq. (3)). All others parameters are identified experimentally and are listed in the Table 1.

The numerical integration requires authors' own algorithm development for the engagement detection inside freewheel, which ensures that the integration procedure does not force infeasible behaviours (e.g. teeth penetration inside freewheel). Should the solution approach the impact zone, when respective tooth and pawl are close to each other, the integration step is reduced in order to accurately detect the beginning of the contact. If the engagement occurs the Eqs. (10a) and (10b) are changed to (5). However, when tooth and pawl are in stick phase, it is checked whether the flywheel shaft drives the pendulum shaft. If this is the case, the integration procedure goes one step back and the equations for the engagement mode Eq. (5) are changed to normal mode Eqs. (10a) and (10b).

In order to explore the dynamics of the system in question, we perform a parameter study in two-parameter space (see Fig. 5). The parameter space is discretised into grid with element size $\Delta\omega = 0.015$ [rad/s], $\Delta A = 5{\cdot}10^{-4}$ [m]. The variable system parameters are set to: $l_{red} = 0.178$ [m], $R_L = 101$ [Ω], while the others remain as listed in Table 1. Each of the elements in the grid is computed starting from the same initial conditions, namely, $\varphi = -\pi/3$, $\dot{\varphi} = 0$, $\theta = 0$, $\dot{\theta} = 0$, $i = 0$. Colour represents maximum peak-to-peak amplitude of pendulum oscillation φ_{pk-pk} detected for time 1000 [s] $< t <$ 1500 [s]. The peak-to-peak amplitude is chosen due to the chaotic and asymmetric oscillation of the pendulum, which is caused mainly by the fact that the freewheel engages only when pendulum is moving in one direction. Red line corresponds to the experimental limit of excitation amplitude $A_{limit} = 0.005$ [m]. The obtained results clearly indicate two resonance tongues. The one for 1:1 resonance is thin and requires excitation amplitude above A_{limit}. Its tip is located at $\omega = 7.41$ [rad] and $A = 0.022$ [m]. On the other hand, the stable region for 2:1 resonance is larger and requires smaller excitation amplitude, suitable for the experimental equipment. This is why in this paper, we focus on the 2:1 resonance only.

In the Figs. 6(a), (c) time diagrams of selected mechanical phase variables are presented, while instantaneous power generated is depicted in Fig. 6(e). The results corresponds to the position of the gravity centre $l = 0.157$ [m], reduced length $l_r = 0.177$ [m], angular excitation frequency $\omega = 14.16$ [rad/s] and electric load $R_L = 48$ [Ω]. Initial conditions used here are as follows: $\varphi = 0.645$ [rad], $\dot{\varphi} = 0$ [rad/s], $\theta = 0$ [rad], $\dot{\theta} = 0$ [rad/s], $i = 0$ [A]. Values of remaining parameters are listed in Table 1.

3.2. Experimental results

An experimental investigation is performed to verify the correctness of the elaborated mathematical model. The experimental rig is depicted in Fig. 3. Two electrical loads (i.e., $R_L = 48$ [Ω], $R_L = 101$ [Ω]) are connected to the generator, in order to compare harvester performance in different working conditions. The whole pendulum set is mounted on a vertical air-cooled LDS low force shaker, oscillating with constant amplitude A. The construction of the pendulum allows to change the position of the pendulum weight, yielding to the variation of reduced length of pendulum l_r. Angular positions and velocities of pendulum and flywheel are extracted by means of motion tracking software, while the current i and output voltage of the generator U is measured using data acquisition card.

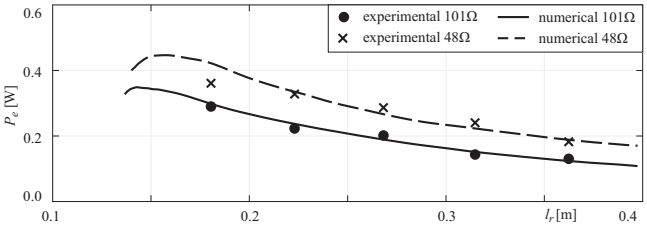

Fig. 7. Effective power as a function of reduced length of the pendulum l_r for different resistors.

Figs. 6(b), (d) present the time diagram for the mechanical phase variables of the system measured in experiment, while instantaneous power generated is depicted in Fig. 6(f). The obtained results are qualitatively comparable with the numerical results presented in Section 3.1. To achieve higher efficiency of energy harvest it is necessary to install high performance electric generator with low mechanical resistance and apply a two directional coupling instead of freewheel mechanism. The device has been additionally tested in real working conditions (see Appendix A).

3.3. Performance optimization

The objective of the optimization is to find the most optimal reduced length of the pendulum l_r for which we can obtain the best power characteristics. Due to the design limit of the experimental set-up we have chosen amplitude of oscillation around 0.87 [rad] as the target. The value of the reduced length of pendulum is changed by changing the position of the pendulum mass along the rod. We have created an algorithm, which calculates the effective power generated for different values of the reduced length of pendulum.

The obtained results are presented in Fig. 7. For each value of reduced length, we find the largest effective power within the amplitude limit of 0.87 [rad]. As the pendulum is in the resonance state, the period of excitation is slowly increased so that it follows the amplitude of oscillation. eventually reaching large values around 0.87 [rad]. After reaching the vicinity of target amplitude algorithm make small changes in the excitation period in order to obtain the largest amplitude possible in that particular range. The system is sensitive to any alterations in the excitation period and it is possible to jump out of the resonance state. Having found the most optimal conditions for particular value of reduced length of pendulum we compute the energy and then the efficient power of the generator according to Eq. (9).

In the Fig. 7 results of parameter study of effective power P_e as a function of reduced length l_r are presented for both, numerical and experimental measurements. The numerical results are depicted with lines, while experimental results with markers. Analysing the results one can conclude that, the most effective value of reduced length is $l_r = 0.153$ [m] for $R_L = 48$ [Ω] and $l_r = 0.143$ [m] for $R_L = 101$ [Ω]. This slight difference is mainly due to different level of damping coefficients c_2 for these resistors. Larger values of reduced length of pendulum produce larger torque transmitted from pendulum to flywheel. However, the longer the pendulum is, the slower it oscillates. The optimal values, which have been found, make balance between the torque driving the generator and speed of oscillation. The experimental results match the results obtained for numerical model qualitatively, as well as quantitatively. We also performed experimental test in water park with artificial waves and we present it Appendix A.

4. Conclusions

In this paper we present device for energy harvesting from pendulum oscillation. A mathematical model is derived, which is then

verified by the performed experiments. The pendulum shows the robustness only at a certain excitation frequency (2:1 locking ratio). The results obtained by the mathematical model qualitatively corresponds to the experimental results. We have found that the energy harvesting is more efficient for shorter reduced length of pendulum (i.e., low excitation and natural periods), which provides large angular velocity crucial to the electric generator, but yet high enough driving torque to overcome friction and damping in the mechanisms. Although, the device fulfilled the main design goal to harvest the pendulum energy, there is still space for improvements (e.g. high performance electric generator, transforming the pendulum movement in both directions, using multiple pendula).

Acknowledgement

This research was supported in part by PL-Grid infrastructure. The paper is also supported in part by the PLATON project's infrastructure at the Lodz University of Technology Computer Centre. Authors would like to thank to Mr. Bogdan Jagiełło for his help in the experiment and Aquapark Fala in Lodz, Poland for possibility of testing device in a wave pool.

PP acknowledges support of Lodz University of Technology Own Scholarship Fund.

Appendix A. appendix

The proposed device has been tested in wave pool in Aquapark Fala in Lodz, Poland. The pendulum is placed in an inflatable boat, equipped with wooden floor, to which the device is mounted. The experiment has shown that the system can work in real environment and the energy generated is enough to power simple LEDs (see Fig. A.1).

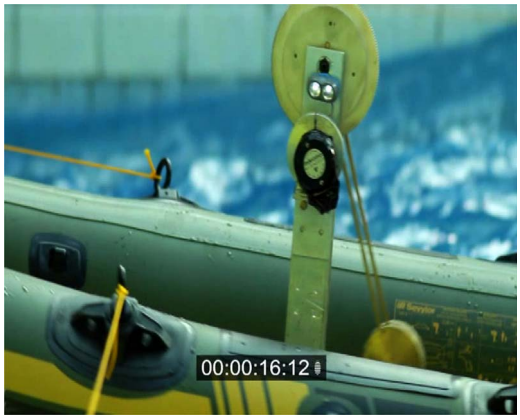

Fig. A.1. Pendulum during tests in wave pool.

References

[1] E.L. Edwardes, The story of the pendulum clock, Sherratt, Altrincham, 1977.
[2] C. Huygens, Horologium oscillatorium: 1673, Dawson, London, 1966.
[3] E.I. Butikov, The rigid pendulum – an antique but evergreen physical model, Eur. J. Phys. 20 (6) (1999) 429–441.
[4] B. Koch, R. Leven, Subharmonic and homoclinic bifurcations in a parametrically forced pendulum, Physica D 16 (1) (1985) 1–13.
[5] A. Skeldon, Dynamics of a parametrically excited double pendulum, Physica D 75 (4) (1994) 541–558.
[6] S. Lenci, G. Rega, Competing dynamic solutions in a parametrically excited pendulum: attractor robustness and basin integrity, J. Comput. Nonlinear Dyn. 3 (4) (2008) 041010.
[7] A.S. de Paula, M.A. Savi, F.H.I. Pereira-Pinto, Chaos and transient chaos in an experimental nonlinear pendulum, J. Sound Vib. 294 (3) (2006) 585–595.
[8] K. Czolczynski, P. Perlikowski, A. Stefanski, T. Kapitaniak, Huygens' odd sympathy experiment revisited, Int. J. Bifurc. Chaos 21 (07) (2011) 2047–2056.
[9] P. Brzeski, P. Perlikowski, S. Yanchuk, T. Kapitaniak, The dynamics of the pendulum suspended on the forced duffing oscillator, J. Sound Vib. 331 (24) (2012) 5347–5357.
[10] M. Kapitaniak, K. Czolczynski, P. Perlikowski, A. Stefanski, T. Kapitaniak, Synchronous states of slowly rotating pendula, Phys. Rep. 541 (1) (2014) 1–44.
[11] B. Witkowski, P. Perlikowski, A. Prasad, T. Kapitaniak, The dynamics of co-and counter rotating coupled spherical pendula, Eur. Phys. J. Spec. Top. 223 (4) (2014) 707–720.
[12] M. Marszal, K. Jankowski, P. Perlikowski, T. Kapitaniak, Bifurcations of oscillatory and rotational solutions of double pendulum with parametric vertical excitation, Math. Probl. Eng. (2014).
[13] F. Reguera, F.E. Dotti, S.P. Machado, Rotation control of a parametrically excited pendulum by adjusting its length, Mech. Res. Commun. 72 (2016) 74–80.
[14] M. Wiercigroch, A New Concept of Energy Extraction from Oscillations via Pendulum Systems, UK Patent Application.
[15] M. Wiercigroch, A. Najdecka, V. Vaziri, Nonlinear dynamics of pendulums system for energy harvesting, in: Vibration Problems ICOVP 2011, Springer, 2011, pp. 35–42.
[16] X. Xu, M. Wiercigroch, M. Cartmell, Rotating orbits of a parametrically-excited pendulum, Chaos Soliton Fractals 23 (5) (2005) 1537–1548.
[17] K. Nandakumar, M. Wiercigroch, A. Chatterjee, Optimum energy extraction from rotational motion in a parametrically excited pendulum, Mech. Res. Commun. 43 (2012) 7–14.
[18] A. Najdecka, S. Narayanan, M. Wiercigroch, Rotary motion of the parametric and planar pendulum under stochastic wave excitation, Int. J. Nonlinear Mech. 71 (2015) 30–38.
[19] S. Lenci, M. Brocchini, C. Lorenzoni, Experimental rotations of a pendulum on water waves, J. Comput. Nonlinear Dyn. 7 (1) (2012) 011007.
[20] G. Rinaldi, A. Fontanella, G. Sannino, G. Bracco, E. Giorcelli, G. Mattiazzo, H. Bludszuweit, Development of a simplified analytical model for a passive inertial system solicited by wave motion, Int. J. Mar. Energy 13 (2016) 45–61.
[21] W.H. Munk, Origin and generation of waves, Coast. Eng. Proc. 1 (1) (2010) 1.
[22] D. Yurchenko, P. Alevras, Dynamics of the n-pendulum and its application to a wave energy converter concept, Int. J. Dyn. Control 1 (4) (2013) 290–299.
[23] P. Alevras, D. Yurchenko, A. Naess, Stochastic synchronization of rotating parametric pendulums, Meccanica 49 (8) (2014) 1945–1954.
[24] P. Alevras, I. Brown, D. Yurchenko, Experimental investigation of a rotating parametric pendulum, Nonlinear Dyn. 81 (1–2) (2015) 201–213.
[25] T. Andreeva, P. Alevras, A. Naess, D. Yurchenko, Dynamics of a parametric rotating pendulum under a realistic wave profile, Int. J. Dyn. Control (2016).
[26] I. Hinck, Wave Power Generator, US Patent 3,231,749, 1966.
[27] S.C. Hench, System and Method for Converting Ocean Wave Energy into Electricity, US Patent 7,737,569, 2010.
[28] S.C. Hench, System and Method for Converting Ocean Wave Energy into Electricity, US Patent 8,046,108, 2011.
[29] H. Paakkinen, Wave Power Plant, EP Patent App. EP20,090,815,731, 2011.
[30] B.C. Boren, B.A. Batten, R.K. Paasch, Active control of a vertical axis pendulum wave energy converter, in: Proceedings of the 2014 American Control Conference (ACC), IEEE, 2014, pp. 1033–1038.
[31] E.S.J. Hesam, B. Ling, B.A. Batten, Use of artificial neural networks for real-time prediction of heave displacement in ocean buoys, in: Proceedings of the 2014 International Conference on Renewable Energy Research and Application (ICRERA), IEEE, 2014, pp. 907–912.
[32] M. Borowiec, G. Litak, A. Rysak, P. Mitcheson, T.T. Toh, Dynamic response of a pendulum-driven energy harvester in the presence of noise, in: Proceedings of the Journal of Physics Conference Series, vol. 476, IOP Publishing, 2013, p. 012038.